

Total Loss Comparison of Inverter Circuit Topologies with Interior Permanent Magnet Synchronous Motor Drive System

Daisuke Sato

Department of Electrical Engineering
Nagaoka University of Technology
Nagaoka, Niigata, Japan
dsato@stn.nagaokaut.ac.jp

Jun-ichi Itoh

Department of Electrical Engineering
Nagaoka University of Technology
Nagaoka, Niigata, Japan
itoh@vos.nagaokaut.ac.jp

Abstract— In this paper, the losses of a drive system for electric vehicles (EVs) which consists of the interior permanent magnet synchronous motor (IPMSM) is analyzed. The applied power converter is distinguished into a 2-level inverter and a 3-level inverter, respectively. In addition, two modulations are applied typically in the inverter, known as Pulse width modulation (PWM) at low speed region and 1-pulse modulation (square wave modulation) at middle or high speed regions. This paper discusses the appropriate interchange point between these modulations in order to achieve minimum loss, by analyzing and comparing the losses for each of the inverter. The total loss is divided into the inverter loss and motor loss, where the inverter loss is calculated by the simulation and the motor loss is analyzed by two-dimensional finite element method (2D-FEM). As a result, the total loss which is composed of the 3-level inverter and the motor losses are shown lower than that of the 2-level inverter. The losses of the 3-level inverter decreases by 5.8% compared to that of the 2-level inverter at base speed. In addition, when the carrier frequency is 5 kHz, the loss of the motor drive system achieves the smallest. Furthermore, the losses of the motor drive system are evaluated by the experiment. According to the results, the high efficiency can be achieved by 1-pulse modulation

Keywords—Interior permanent magnet synchronous Motor; 3-level inverter; 1-pulse modulation; High efficiency drive

I. INTRODUCTION

Recently, the electric vehicles (EV) are actively developed due to the high demand from automobile industry intends to reduce the CO₂ emission. The typical motor applied in EVs is the interior permanent magnet synchronous motor (IPMSM), which features lightweight, high power density and high efficiency [1-4]. Then, a 2-level inverter is applied to control the torque in a wide range of a variable speed.

The inverter in an EV system is typically driven by two modulations, that is, PWM at low speed region and 1-pulse modulation (square wave modulation) at middle or high speed regions [5-6]. PWM can suppress the torque ripple because the harmonic component is relatively low. Then, the implementation of 1-pulse modulation can increase the fundamental amplitude of the output voltage and also reduce

the switching loss comparing with that of PWM. Hence, the 1-pulse modulation is often applied to extend the speed range.

On the other hand, the multilevel inverter as typified by a 3-level inverter is an alternative converter from the typical 2-level inverter [7]. The 3-level inverter can reduce a harmonic component of voltage comparing to the 2-level inverter due to the possible to output zero voltage level. In motor drive systems, high efficiency is expected by implementing the multilevel inverter because the harmonic loss of the motor is reduced.

In addition, the pulse width of the 1-pulse modulation can be varied in a 3-level inverter unlike the 2-level inverter because the 3-level inverter can output zero voltage level. As a result, it can arbitrarily decide the fundamental amplitude of output voltage and it is so called as the “1-pulse modulation” in order to distinguish from the standard 1-pulse modulation [8]. However, there is an interchange point from PWM to 1-pulse modulation. In order to achieve the highest efficiency, the interchange point is required to further analyze under different conditions. Here, the selection method of the interchange point considers the losses from both the PWM and 1-pulse modulation at same motor speed and loads. The modulation that produces the smallest loss in each operation region will be selected to achieve high efficiency.

The study of loss analysis of the inverter loss or the IPMSM loss has been individually reported in [9-13]. However, the evaluation on losses of the total drive system that includes the inverter and IPMSM has not been reported for the purpose of selecting the optimal operation method.

In this paper, the total loss of the IPMSM drive systems is analyzed and measured by using a 2-level inverter and a 3-level inverter, respectively. In addition, this paper discusses the interchange point between modulations in order to achieve the minimum loss, by analyzing and comparing the losses for each operation of the inverters. The total losses of the drive system are subjected to the motor speed and carrier frequency. The total losses are divided into the inverter loss and the motor loss. Firstly, breakdowns of losses for the inverter are demonstrated when the distributed winding IPMSM is driven. Secondly, the

loss of the distributed winding IPMSM is analyzed by two-dimensional finite element method electromagnetic field analysis (FEM). In addition, the total loss of the distributed winding IPMSM drive system analysis result will clearly demonstrate the relationship between the operation method and the total loss. Finally, the concentrated winding IPMSM drive system by using the 3-level inverter is demonstrated in order to measure the loss of the motor drive system at different carrier frequencies for PWM and 1-pulse modulation.

II. MOTOR DRIVE SYSTEM CONFIGURATION

Fig. 1 shows circuit diagrams of each inverter. A 3-level T-type inverter can reduce a harmonic component of the output current and voltage compared to the 2-level inverter since the output voltage has three levels, hence, the motor loss can be reduced. Furthermore, the switching loss can be reduced because the carrier frequency of the 3-level inverter is lower than that of the 2-level inverter when achieving the same harmonic components. In addition, the conduction loss of the 3-level inverter is approximately the same as that of the 2-level inverter because the number of the switching devices which the current passes through in the 3-level inverter is similar to that of the 2-level inverter.

Fig. 2 shows the relationship between the motor speed and the inverter output voltage. Operating areas A and B is the PWM region for the 2-level inverter. However, for the 3-level inverter, area B is the 1-pulse modulation region and the switching loss can be reduced in this region.

At the 1-pulse modulation, the fundamental voltage amplitude is decided by zero-level phase α , and fourier series expansion of U-phase voltage v_u is expressed by (1).

$$v_u = \sum_{n=1}^{\infty} \left[\frac{2E_{dc}}{(2n-1)\pi} \cos\{(2n-1)\alpha\} \sin\{(2n-1)\omega t\} \right] \\ = \frac{2E_{dc}}{\pi} \cos \alpha \sin \omega t + \frac{2E_{dc}}{3\pi} \cos(3\alpha) \sin(3\omega t) \quad (1), \\ + \frac{2E_{dc}}{5\pi} \cos(5\alpha) \sin(5\omega t) + \dots$$

where E_{dc} is the DC voltage of the inverter, ω is the electrical angular frequency. Furthermore, the fundamental voltage amplitude can be calculated from the first term of (1). If $\alpha = 0$, the operation method becomes 1-pulse modulation as shown in area C (Fig. 2) because the output voltage is saturated.

Fig. 3 shows the relationship between torque and speed of the distributed winding IPMSM for the EVs. The based speed of the IPMSM is 2768 r/min, the maximum speed is five times of the based speed (13900 r/min) and the rated torque is 207 Nm. In this paper, the operation point to compare total loss is shown as N-T map in Fig. 3.

III. INVERTER LOSS ANALYSIS

A. Loss Calculation of Inverter

In this section, the loss calculation method for an inverter is described. The inverter loss P_{inv} is separated into follows: the conduction loss of IGBTs P_{con_IGBT} , the conduction loss of

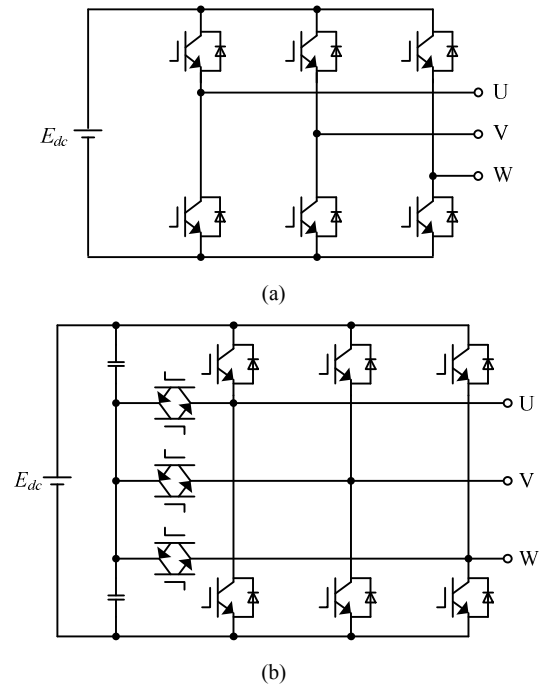


Fig. 1. Circuit diagrams of each inverter. (a) 2-level inverter. (b) 3-level T-type NPC inverter. A 3-level T-type inverter can reduce a harmonic component of the output current and voltage compared to the 2-level inverter.

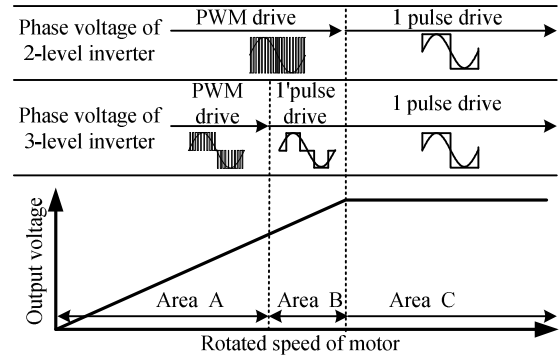


Fig. 2. Comparison of operation method each inverter circuit. When the motor speed is low (at Area A), the inverter is operated by PWM. At middle speed (Area B), the 3-level inverter can be operated by 1-pulse modulation. At high speed (Area C), 1-pulse modulation is selected.

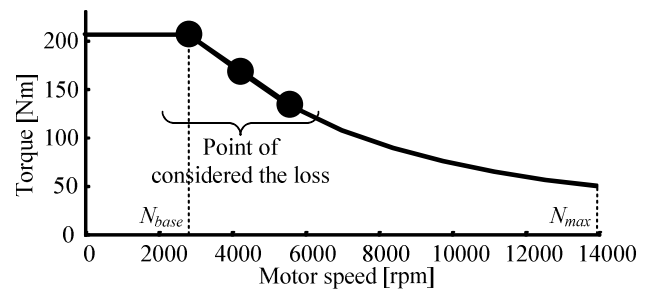


Fig. 3. Torque and speed characteristic of the IPMSM for the EVs. The maximum speed is five times of the base speed. In this paper, the loss of the drive system is considered at three points in this figure.

TABLE I. PARAMETERS OF THE DISTRIBUTED WINDING IPMSM.

Rated power P_r	60 kW
DC link voltage E_{dc}	650 V
Rated Torque T_r	207 Nm
Base speed N_{base}	2768 r/min
Maximum speed N_{max}	13900 r/min
Rated Current I_n	141 Arms
Armature pairs of poles p	4
d-axis inductance L_d	0.554 mH
q-axis inductance L_q	1.662 mH
Winding resistance R_a	0.0789 Ω (20 deg.)
Back-emf coefficient Φ	0.0845 Vs/rad

diodes P_{con_D} , the switching loss of IGBT P_{sw} and the recovery loss of diode P_{rec} . The inverter loss P_{inv} is expressed by (2).

$$P_{inv} = P_{con_IGBT} + P_{con_D} + P_{sw} + P_{rec} \quad (2)$$

The conduction loss P_{con} can be calculated by integrating the product of current flowing along elements i_{sw} and the on-voltage v_{on} under the conduction time from θ_1 to θ_2 (θ_1 is the phase angle when the current begins to flow through the IGBT. θ_2 is the phase angle when the current finishes to flow.). The conduction loss P_{con} is expressed by (3).

$$P_{con} = \frac{1}{2\pi} \int_{\theta_1}^{\theta_2} v_{on} i_{sw} d\theta \quad (3)$$

The switching loss is proportional to the current flows via elements and the voltage applied to elements. Additionally, the applied voltage to the IGBTs is constant. Therefore, the average switching loss during output cycle is expressed by (4).

$$P_{sw} = E_{dc} (e_{on} + e_{off}) f_c \frac{1}{2\pi} \int_{\theta_1}^{\theta_2} i_{out} d\theta \quad (4),$$

where, f_c is the carrier frequency, E_{dc} is the DC voltage and i_{out} is the output current. Furthermore, e_{on} is the turn-on energy when the current flowing along IGBTs is 1A and the voltage applied to IGBTs is 1 V. e_{off} is the turn-off energy.

The recovery loss of the freewheeling diode P_{rec} is expressed by (5).

$$P_{rec} = E_{dc} e_{rr} f_c \frac{1}{2\pi} \int_{\alpha}^{\beta} i_{out} d\theta \quad (5),$$

where, e_{rr} is the recovery loss energy.

B. Loss Calculation Results of Each Inverter

The loss of the 2-level inverter and the 3-level inverter is calculated based on following conditions. The output power is decided from the rated current and the carrier frequency f_c is 5 kHz and 10 kHz for PWM drive, respectively. In addition, the modulation strategy for the 3-level inverter is applied with a unipolar modulation. The IGBT models are 6MBI300V-120-50 (1200V, 300A) from Fuji Electric Corp. Table I shows the parameters of the distributed winding IPMSM that referred to Refs. [14-15].

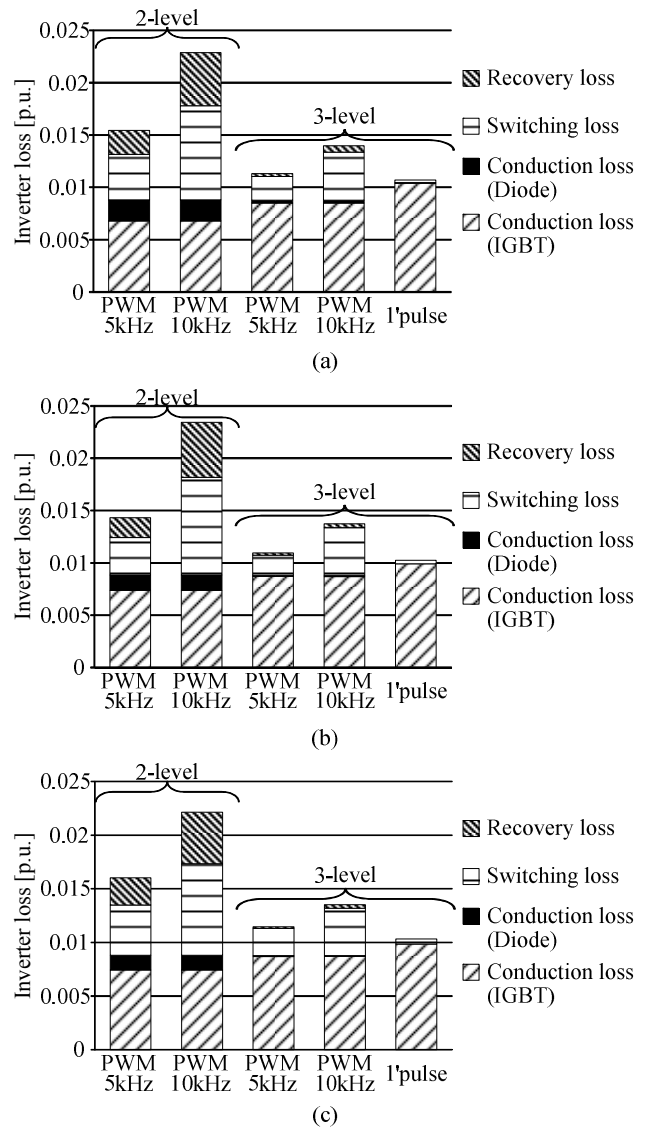


Fig. 4. Inverter loss analysis results for each operation condition. (a) Motor speed at 2768 r/min (base speed). (b) Motor speed at 4170 r/min. (c) Motor speed at 5560 r/min. The loss of 1'pulse modulation is the smallest. In addition, the loss of the 3-level inverter (PWM 5 kHz) at 2768 r/min decreases by 26.6% compared to that of the 2-level inverter (PWM 5 kHz).

Fig. 4 shows the detail breakdown of the inverter losses. The loss is standardized by the rated motor power. In PWM drive, the loss at $f_c = 5$ kHz is the smallest in each inverter because the switching loss increases in proportional to the carrier frequency. On the other hand, the losses produced from 1'pulse modulation is shown smaller than the PWM drive in all speed range because the switching frequency is the same as the output frequency, i.e. it is the lowest. In addition, the switching loss of the 3-level inverter is half of that of the 2-level inverter due to the reason that the average voltage of the IGBT is half of the 2-level inverter in a voltage phase period.

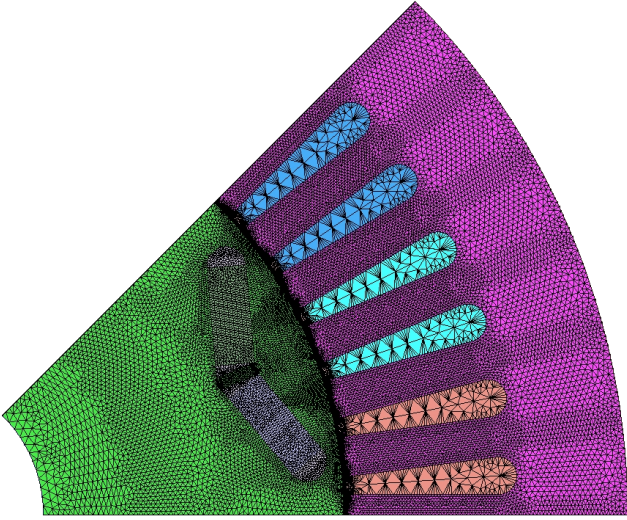


Fig. 5. 2D-FEM model of the distributed winding IPMSM. The model is divided into one of the eighth in a circumferential direction.

TABLE II. CONDITION OF THE DISTRIBUTED WINDING IPMSM LOSS ANALYSIS USING FEM.

Core (rotor, stator)	35JN300 / JFE Steel
Magnet	NMX-39EH / Hitachi Metals
Coil turns per phase	11 Turns
Outer diameter of stator	264 mm
Iron stack length	50 mm
Number of elements	38842
Time interval per 1 step	10 μ s
Computer	Xeon X5450 3.0GHz

IV. MOTOR LOSS ANALYSIS

The motor loss can be classified into three categories: (i) a copper loss by a wiring resistance, (ii) an iron loss generated in a rotor core, a stator core and a magnet and (iii) the mechanical loss. In this section, the mechanical loss is ignored because this loss is depending on a motor speed. The motor loss is analyzed by two-dimensional finite element method electromagnetic field analysis (FEM) using JMAG (JSOL). The FEM analyzes the magnetic field generated in the motor, and then the losses are calculated based on the results. At first, the two-dimensional model of the motor is developed. Next, the loss analysis is performed by inputting the current waveform which is obtained from the simulation.

Fig. 5 shows the distributed winding IPMSM model and Table II shows the condition of the IPMSM loss analysis using FEM. The model is divided into one of the eighth in a circumferential direction. It is noted that the layout of the magnet is V-shaped and it is divided because the large reluctance torque is generated.

Fig. 6 shows the breakdown of the motor loss, similar to Fig. 4, the results are standardized by the rated motor power. From Fig. 6, the motor losses are dominated by the copper loss. The loss at 1'pulse modulation is shown to be the largest because the harmonic components in the output voltage and the current of the 1'pulse modulation are larger than that of the PWM drive. As a result, the eddy-current generated in cores

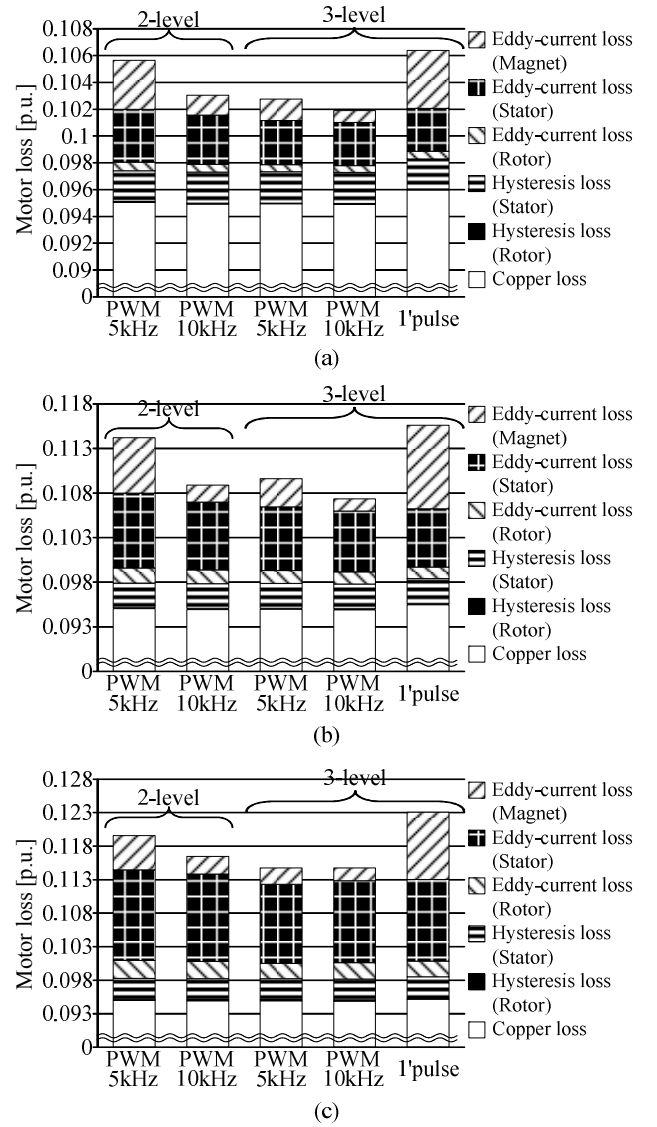


Fig. 6. Motor loss analysis results for each operation conditions. (a) Motor speed at 2768 r/min (base speed). (b) Motor speed at 4170 r/min. (c) Motor speed at 5560 r/min. The loss of the 3-level inverter (PWM 10 kHz) is the smallest. In addition, the loss of the 3-level inverter (PWM 5 kHz) at 2768 r/min decreases by 2.7% compared to that of the 2-level inverter (PWM 5 kHz).

and the magnetics becomes higher, and the eddy-current loss is also increased. In addition, the eddy-current loss in magnet is decreased with the increasing the carrier frequency. Especially, in the 2-level inverter, the variation of the eddy-current loss in the magnet is large. From this result, a 2-level inverter is susceptible to the carrier frequency.

V. DISCUSSIONS OF TOTAL LOSSES

From the analysis results, the total loss of the drive system can be demonstrated, and the next step will consider the optimal operation point for each of the inverter topology.

Fig. 7 shows the relationship between the motor speed and the total loss. From Fig. 7, the loss generated in the 3-level inverter is lower than that in the 2-level inverter. The loss of

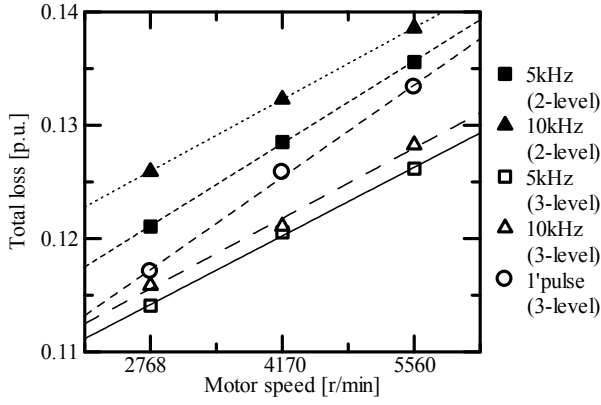


Fig. 7. Total loss of the distributed winding IPMSM drive system. The total loss of the 3-level inverter (PWM5kHz) is the smallest. At base speed (2768 r/min), the total loss of the 3-level inverter decrease by 5.8% compared to that of the 2-level inverter.

the 3-level inverter ($f_c = 5$ kHz) decreases by 5.8% compared to that of the 2-level inverter ($f_c = 5$ kHz) at 2768 r/min (base speed). Therefore, in order to achieve high efficiency, the 3-level inverter is a better option to apply in an IPMSM drive system for EVs. In addition, from Fig. 4 and Fig. 6, the inverter loss of this drive system is quite smaller than the motor loss. Therefore, if the 3-level inverter is applied, it is more effective to reduce the switching loss by the 1'pulse modulation than to reduce the harmonic loss of the motor by the PWM drive.

From Figs. 4 and 6, the relationship between the carrier frequency and the loss of the motor drive system becomes obvious. As a result, the losses of the drive system can be classified into the following three categories,

- The loss that unrelated to the carrier frequency (ie, the copper loss, the iron loss and the conduction loss by the fundamental component).
- The loss that increases subject to the carrier frequency P_s (ie, the switching loss and the recovery loss, also known as inverter loss).
- The loss that increases subject to the carrier frequency P_h (the copper loss, the iron loss and the conduction loss by the harmonic component).

If the carrier frequency of the minimum loss is selected, only P_s and P_h are considered. In other words, when the sum of P_s and P_h (P_v) become minimum, the optimal efficiency driving point can be achieved.

Fig. 8 shows the loss P_s , the loss P_h that subjected to the carrier frequency and the sum value $P_v = P_s + P_h$ at 2768 r/min. From Fig. 8, P_s increases linearly to the carrier frequency because the switching and the recovery losses are proportional to the carrier frequency. In addition, P_h decreases non-linearly. This reason is that the harmonic component in output current is changing non-linearly to the carrier frequency. Furthermore, from the curve of P_v , it is confirmed that the carrier frequency at 3700 Hz can achieve the lowest losses.

Fig. 9 shows the curves of P_v at different operating speed. From Fig. 9, the minimum loss point is changed in subjecting

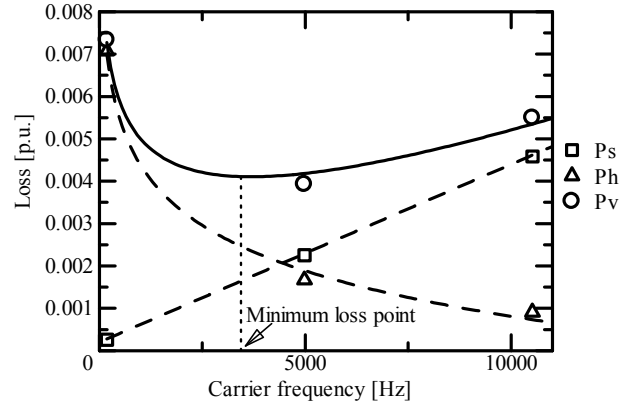


Fig. 8. The increasing loss P_s and the decreasing loss P_h with the rising carrier frequency and the sum value P_v at 2768 r/min. P_s increases linearly and P_h decreases non-linearly for the carrier frequency. The carrier frequency at 3700 Hz can achieve the lowest losses

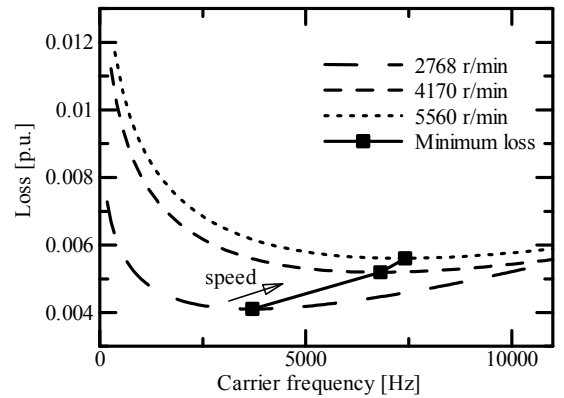


Fig. 9. The curves of P_v at different operating speed. The minimum loss point is changed in subjecting to the motor speed.

to the motor speed. In addition, if the carrier frequency is changed along with the motor speed, the point that can achieve the minimum loss is change accordingly. Furthermore, in Fig. 9, the carrier frequency that can achieve the minimum loss increasing as the motor speed is increasing. In another words, this result means that the ratio of the motor loss in the total loss of the drive system is higher than that of the inverter loss.

VI. EXPERIMENTAL EVALUATION

A. Configuration of Experimental Installation

The concentrated winding IPMSM drive system that is driven by the 3-level inverter is built in order to evaluate the proposed method that achieves the minimum loss in section V by the experimental results.

Fig. 10 shows a configuration of the prototype drive system and Table III shows the parameters of the concentrated winding IPMSM. The IGBT switching devices that applied in the 3-level inverter are 2MB1150U2A-060 (600V, 150A) from Fuji Electric Corp. In addition, the power consumption of the inverter is measured by the power meter (WT1800 / YOKOGAWA). The measurement points for the inverter are between the DC bus capacitor and the output of the inverter.

Furthermore, the torque meter is connected between the IPMSM and the permanent magnet synchronous generator.

The output torque is adjusted by the load resistance. For the control of motor, PWM is implemented with the field oriented control and maximum torque per ampere control. Then, a balance control is applied to balance the two DC capacitors at DC link. At 1'pulse modulation, a V/f control with a stabilization control is applied.

Fig. 11 shows the U-V line-to-line voltage and U phase current waveforms of the 1'pulse modulation. From Fig. 11, it is noted that the current waveform is distorted because the IPMSM is a concentrated windings and a back electromotive force of the motor contains harmonic components. In addition, the reason includes that the inductance of the motor is smaller than that of typically PMSMs.

B. Measurement Results of the Total loss in the IPMSM Drive System

Fig. 12 shows the loss measurement results of the prototype IPMSM drive system. The loss is standardized by the rated motor power. Here, the ratio between the switching losses and conduction losses is set by the carrier frequency similar to Fig. 4. In addition, "PWM1" and "PWM2" are related to the carrier frequency 5 kHz and 10 kHz in Fig. 4, respectively. From Fig. 12, it is confirmed that the loss of the 1'pulse modulation is lower than that of the PWM. Especially, the loss of the 1'pulse modulation is 16% smaller than that of PWM2 at 0.5 p.u.. This reason is that the ratio of the switching loss in PWM is larger

than that of the losses by the harmonic components in 1'pulse modulation.

The proposed method that achieves the minimum loss operation described in section V is evaluated. The curve of P_v is obtained from the experimental results.

Fig. 13 shows the curves of P_v at different operating speed by the measurement results of the total loss. From Fig. 13, it is confirmed that the 1'pulse modulation is the lowest P_v at each motor speed. In addition, the total loss of the drive system is the lowest at 1'pulse modulation from Fig. 12. Thus, the minimum point of P_v and the total loss of the drive system are conformable. As a result, the validity of the proposed method is confirmed. Furthermore, the relationship between P_v and the carrier frequency is different compared to Fig. 9. This reason is that the effect of the switching loss is larger than that of the loss of the harmonic component.

VII. CONCLUSION

In this paper, the losses of two inverter topologies are considered in order to achieve high efficiency for the interior permanent magnet synchronous motor drive system. As a result, the total loss which is consisted from the inverter and the motor losses of the 3-level inverter are lower than that of the 2-level inverter. The loss of the 3-level inverter decreases by 5.8% compared to that of the 2-level inverter at base speed. Therefore, the 3-level inverter is suitable for the drive system in order to achieve the high efficiency. In addition, the optimal operation point for the 3-level inverter is considered by the loss analysis results. As a result, it proves that only the losses that increase and decrease subject to the carrier frequency is considered. Finally, the loss of the other motor drive system is measured by the experimental and the availability of the proposed method is evaluated. As a result, the loss of the drive system at 1'pulse modulation is smallest and the proposed method also same result. In the future work, the calculation for a motor loss will be simplified.

REFERENCES

- [1] Pellegrino G., Vagati A., Guglielmi P. and Boazzo B., "Performance Comparison Between Surface-Mounted and Interior/min Motor Drives for Electric Vehicle Application", IEEE Transactions on Industrial

TABLE III. PARAMETERS OF THE CONCENTRATED WINDING IPMSM.

Rated power P_r	3 kW
DC link voltage E_{dc}	180 V
Rated Torque T_r	4 Nm
Base speed N_{base}	7200 r/min
Maximum speed N_{max}	12000 r/min
Rated Current I_n	16.9 Arms
Armature pairs of poles p	6
d-axis inductance L_d	0.389 mH
q-axis inductance L_q	0.556 mH
Winding resistance R_a	0.0635 Ω (20 deg.)
Back-emf coefficient Φ	0.0182 Vs/rad

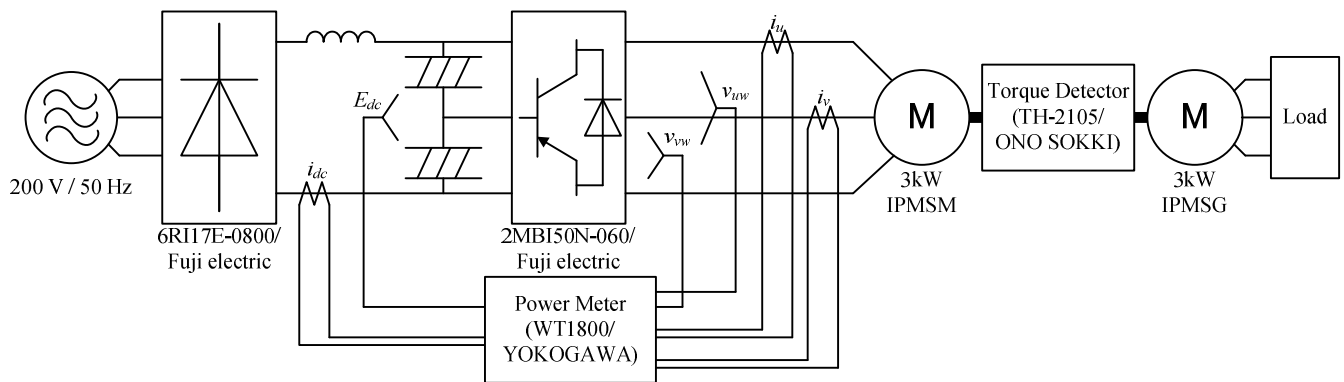


Fig. 10. Configuration of the prototype drive system. The 3-level inverter consists of the IGBT (2MB150N-060, Fuji electric). The output torque is adjusted by the load resistance. The motor control method at PWM uses a field oriented control with a maximum torque per ampere control and a balance control is applied. At 1'pulse modulation, a V/f control with a stabilization control is applied. The loss of the inverter is measured by the power meter (WT1800 / YOKOGAWA). In addition, the shaft output of the IPMSM is measured by the torque detector (TH-2105 / ONO SOKKI).

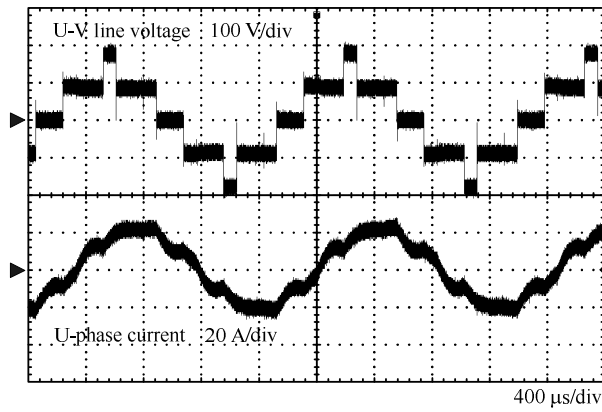


Fig. 11 U-V line-to-line voltage and U phase current waveforms of the 1'pulse modulation. The current waveform is distorted because the IPMSM is a concentrated windings and back electromotive force of the motor contains harmonic component.

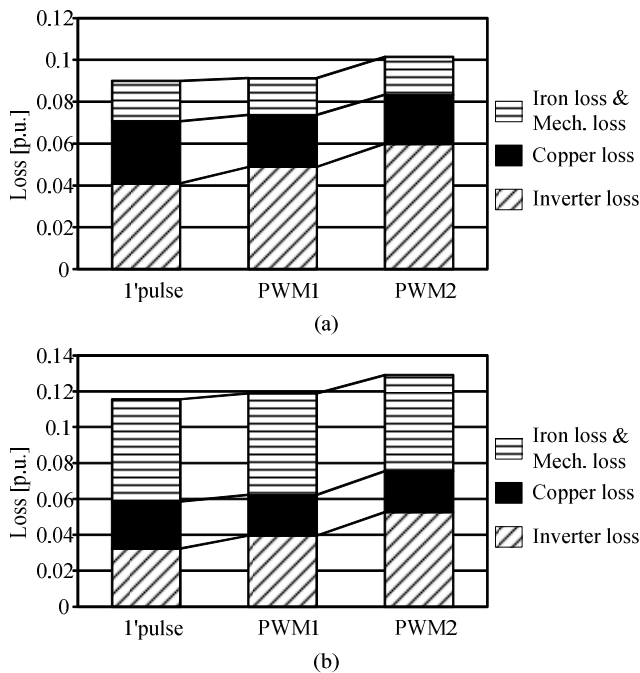


Fig. 12 Loss measurement results of developed IPMSM drive system. (a) Motor speed at 0.2 p.u. (b) Motor speed at 0.5 p.u. The ratio between the switching and conduction losses is similar to Fig. 4. "PWM1" and "PWM2" are related to the carrier frequency 5 kHz and 10 kHz in Fig. 4, respectively. The loss of the 1'pulse modulation is 16% smaller than that of the PWM2 at 0.5 p.u.. The ratio of the switching loss in PWM is larger than that of the losses by the harmonic components in 1'pulse modulation.

Electronics, Vol.59, No.2, pp.803-811 (2012).

- [2] X. Yuan, J. Wang, "Torque Distribution Strategy for a Front- and Rear-Wheel-Driven Electric Vehicle", IEEE Transactions on Vehicular Technology, Vol.61, No.8, pp.3365-3374 (2012).
- [3] David G. Dorrell, Andrew M. Knight, Lyndon Evans, Mircea Popescu, "Analysis and Design Techniques Applied to Hybrid Vehicle Drive Machines—Assessment of Alternative IPM and Induction Motor Topologies", IEEE Transactions on Industrial Electronics, Vol.59, No.10, pp.3690-3699 (2012).
- [4] Ruiwu Cao, Chris Mi, Ming Cheng, "Quantitative Comparison of Flux-Switching Permanent-Magnet Motors With Interior Permanent Magnet

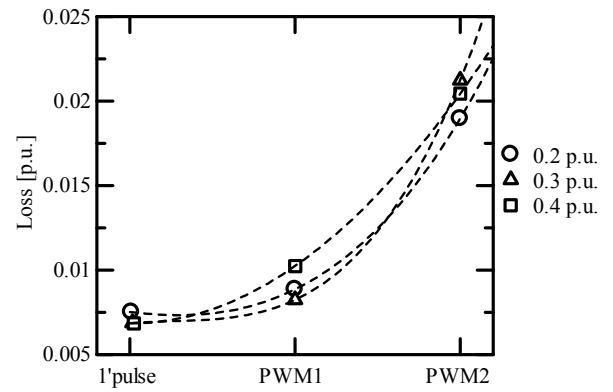


Fig. 13. The curves of P_i at different operating speed by the measurement results. The 1'pulse modulation can achieve the lowest losses because the effect of the switching loss is larger than that of the loss of the harmonic component.

Motor for EV, HEV, and PHEV Applications", IEEE Transactions on Magnetics, Vol.48, No.8, pp.2374-2384 (2012).

- [5] H. Nakai, H. Ohtani, Eiji Satoh and Y. Inaguma, "Development and Testing of the Torque Control for the Permanent-Magnet Synchronous Motor", IEEE Transactions on Industry Applications, Vol.52, No.3, pp.800-806 (2005).
- [6] Y. Nakazawa, S. Toda, I. Yasuoka, H. Naito, "One-Pulse PWM Mode Vector Control for Traction Drives", IEEE Power Electronics in Transportation, pp.135-141 (1996).
- [7] A. Nabae, I. Takahashi and H. Akagi, "A New Neutral-Point-Clamped PWM Inverter," IEEE Transactions on Industry Applications, Vol. IA-17, No.5, pp.518-523 (1981).
- [8] K. Kondo, K. Matsuoka, Y. Nakazawa, "A Designing Method in Current Control System of Permanent Magnet Synchronous Motor for Railway Vehicle Traction", T. IEE Japan, Vol.118-D, No.7-8, pp.900-907 (1998) (in Japanese).
- [9] Y. Kawase, T. Yamaguchi, T. Umemura, Y. Shibayama, K. Hanaoka, S. Makishima and K. Kishida, "Effects of Carrier Frequency of Multilevel PWM Inverter on Electrical Loss of Interior Permanent Magnet Motor", ICEMS2009, LSSA-2 (2009).
- [10] T. Okitsu, D. Matsubashi, K. Muramatsu, "Method for Evaluating the Eddy Current Loss of a Permanent Magnet in a PM Motor Driven by an Inverter Power Supply Using Coupled 2-D and 3-D Finite Element Analyses", IEEE Transactions on Magnetics, Vol.45, No.10, pp.4574-4577 (2009).
- [11] K. Yamazaki, Y. Fukushima, M. Sato, "Loss Analysis of Permanent-Magnet Motors With Concentrated Windings—Variation of Magnet Eddy-Current Loss Due to Stator and Rotor Shapes", IEEE Transactions on Industry Applications, Vol.45, No.4, pp.1334-1342 (2009).
- [12] S. Dieckerhoff and S. Bernet, "Power Loss-Oriented Evaluation of High Voltage IGBTs and Multilevel Converters in Transformerless Traction Applications", IEEE Transactions on Power Electronics, Vol.20, No.6, pp.1328-1336 (2005).
- [13] Ke Ma, Frede Blaabjerg, "Loss and Thermal Redistributed Modulation Methods for Three-level Neutral-Point-Clamped Wind Power Inverter Undergoing Low Voltage Ride Through", ISIE2012, pp.1880-1887 (2012).
- [14] T. A. Burriss, S. L. Campbell, C. L. Coomer, C. W. Ayers, A. A. Wereszczak, J. P. Cunningham, L. D. Marlino, L. E. Seiber, H. T. Lin, "Evaluation of the 2010 Toyota Prius Hybrid Synergy Drive System", ORNL/TM-2010/253, (2010).
- [15] K. Kiyota, H. Sugimoto, A. Chiba, "Comparison of Energy Consumption of SRM and IPMSM in Automotive Driving Schedules", ECCE2012, pp.853-860 (2012).